Higher harmonic instability of electrostatic ion cyclotron waves

T SREERAJ ⬤ *, S V SINGH and G S LAKHINA

Indian Institute of Geomagnetism, Plot 5, Sector 18, Near Kalamboli Highway, New Panvel (W),
Navi Mumbai 410 218, India
*Corresponding author. E-mail: sreerajt90@gmail.com

Abstract. Electrostatic ion cyclotron instability pertaining to the higher harmonics of proton and helium cyclotron modes is investigated in three-component magnetised plasma consisting of beam electrons, protons and doubly charged helium ions. The effect of different plasma parameters, namely, angle of propagation, number density and temperature of helium ions and electron beam speed, has been studied on the growth of proton and helium cyclotron harmonics. It is found that an increase in angle of propagation leads to the excitation of fewer harmonics of proton cyclotron waves with decreased growth rates and higher number of helium harmonics with decreased growth rates. Also, largely odd helium harmonics are excited, except for one particular case where the second harmonic also becomes unstable. The number density and temperature of ions have significant effect on the helium cyclotron instability compared to the proton cyclotron instability. Further, as the speed of electron beam is increased, the peak growth rate increases. Our results are relevant to laboratory and space plasmas where field-aligned currents exist.

Keywords. Electrostatic ion cyclotron instability; space plasma; ionosphere; kinetic theory.

PACS Nos 52.25.Dg; 52.25.Xz; 52.35.−g; 52.35.Fp

1. Introduction

Electrostatic ion cyclotron (EIC) waves were first observed in laboratory plasma, comprising cesium and potassium by D'Angelo and Motley [1] and Motley and D'Angelo [2]. These waves propagate nearly perpendicular to the ambient magnetic field, with a small finite wave number along the ambient magnetic field. EIC instability in the ionosphere and magnetosphere can arise from different free energy sources such as field-aligned currents, ion beams, velocity shear, relative streaming between ions, electron drifts and density gradients [3–15]. EIC waves have been studied in plasmas having heavy metallic ions or dust grains [16–23]. In Aditya tokamak, Chattopadhyay *et al* [24] have studied the second-harmonic ion cyclotron resonance heating. EIC waves have been observed in high-latitude ionosphere [25]. Many spacecraft observations, e.g. S3-3 [9,26,27], GEOS 1 and 2 satellites [28,29], ISEE-1 [30], Viking [31], Polar [32], FAST [33] and THEMIS [34] have shown the presence of EIC waves in different regions of Earth's magnetosphere. EIC waves serve as the main source for ion heating in magnetosphere. Therefore, they have been of great interest to the space plasma community. Dakin *et al* [35] demonstrated that

significant ion heating can occur by EIC modes excited by electron current. Ungstrup *et al* [36] found that EIC waves heat up the ions to superthermal energies transverse to the Earth's magnetic field. Roux *et al* [29] also observed heating of He$^+$ ions associated with EIC waves in the magnetospheric region.

The presence of heavy ions has been confirmed in space plasmas. For example, the presence of α (He^{2+}) particles precipitating into the nightside auroral zone on a satellite pass over the southern hemisphere on 16 May 1972 during a magnetic storm has been recorded [37]. These α-particles are of solar wind origin and are about 4% of the proton density. Recently, Tang *et al* [34] observed EIC waves at fundamental and second harmonic of proton and at doubly charged helium cyclotron frequencies which establish the presence of He^{2+} ions in the magnetopause. Helium and oxygen are often seen inside the magnetopause and adjacent to it. However, the THEMIS mission does not make ion composition measurements to distinguish different ion species. The doubly charged helium is of solar wind origin and hence density will be low (<5% or so). Recently, Sreeraj *et al* [38,39] have studied the ion cyclotron and ion-acoustic waves in the solar wind and lunar wake plasmas in the presence of doubly charged helium.

Therefore, it is important to study EIC instabilities involving He^{2+} ions which are of solar wind origin and are found in various regions of the Earth's magnetosphere and can impact the growth of EIC waves. In this paper, instability of higher harmonic of electrostatic proton and helium cyclotron waves is studied using the kinetic theory in a three-component magnetised plasma comprising drifting electrons, Maxwellian protons and doubly charged helium ions. Although the focus of the paper is not particularly to explain any specific observation, our results will be useful in understanding EIC instabilities in laboratory and space plasmas where field-aligned currents exist. Theoretical model and the dispersion relation are presented in §2. In §3, numerical results are presented and conclusion and discussion are given in §4.

2. Theoretical model

We consider collisionless, three-component magnetised plasma composed of electrons, protons and doubly charged helium ions. The electrons are assumed to stream with speed U_b along the ambient magnetic field, $\mathbf{B_0} \| \hat{z}$. Here, protons and helium follow Maxwell distribution ($U_p = U_\alpha = 0$) whereas electrons are having a drifting Maxwellian (U_b is non-zero) distribution. The low-frequency electrostatic waves are considered to be propagating in the x–z plane with wave vector, $\mathbf{k} = k_\perp \hat{x} + k_\| \hat{z}$; $k_\|$ and $k_\perp$ are the parallel and perpendicular wave numbers, respectively. The dispersion relation for the electrostatic waves in magnetised plasma can be written as [5]

$$D(\omega, k) = 1 + \sum_s \chi_s$$
$$= 1 + \sum_s \frac{1}{k^2 \lambda_{Ds}^2}$$
$$\times \left[1 + \sum_{n=-\infty}^{\infty} \frac{\omega - k_\| U_s}{\sqrt{2} k_\| v_{ts}} \Gamma_n(b_s) Z(\xi_{ns}) \right], \quad (1)$$

where χ_s is the susceptibility of the species s and subscripts $s = e, p, \alpha$ refer to electron, proton and doubly charged helium ions, respectively. The argument of the plasma dispersion function ξ_s is given by

$$\xi_{ns} = \frac{\omega - n\Omega_s - k_\| U_s}{\sqrt{2} k_\| v_{ts}}. \quad (2)$$

For wave frequency ω much less than electron cyclotron frequency, the maximum contribution for electrons will come from $n = 0$ terms and hence, susceptibilities for electrons can be written as [19,20,22]

$$\chi_e \approx \frac{1}{k^2 \lambda_{De}^2} \left[1 + \frac{\omega - k_\| U_b}{\sqrt{2} k_\| v_{te}} \Gamma_0(b_e) Z(\xi_{0e}) \right]. \quad (3)$$

Here, $\lambda_{Ds} = v_{ts}/\omega_{ps}$, $\omega_{ps} = \sqrt{z_s^2 n_{0s} q_s^2 / \epsilon_0 m_s}$, $\Omega_s = z_s q_s B_0 / m_s$, U_s and $v_{ts} = \sqrt{T_s/m_s}$ are the Debye length, plasma frequency, cyclotron frequency, beam and thermal velocity of the sth species, respectively, ϵ_0 is the permittivity of the free space, m_s, z_s and q_s are, respectively, the mass, atomic number and charge of the sth species, $\Gamma_n(b_s) = I_n(b_s) \exp(-b_s)$, where $I_n(b_s)$ is the modified Bessel function of order n with its argument $b_s = k_\perp^2 v_{ts}^2 / \Omega_s^2$ and Z is the plasma dispersion function. To arrive at eq. (3), we have used the fact that Larmor radius of the electron is small with $b_e \ll 1$. As $b_e \ll 1$, we retain only $n = 0$ term as $\Gamma_0(0) = 1$ and $\Gamma_n(0) = 0$ for all $n \neq 0$. Assuming $\omega = \omega_r + i\gamma (\gamma \ll \omega_r)$, the dispersion relation given by eq. (1) can be written as

$$D_r(\omega_r, k) + i D_i(\omega_r, k) = 0, \quad (4)$$

where D_r and D_i are the real and imaginary parts of the dispersion relation, eq. (1). The growth or damping of the low-frequency wave is given by

$$\gamma = -\frac{D_i(\omega_r, k)}{\partial D_r(\omega_r, k)/\partial \omega_r}. \quad (5)$$

Analytical results on proton cyclotron harmonics are presented in the next subsection.

2.1 *Proton cyclotron harmonics*

In this subsection, we study the instability associated with proton cyclotron harmonics. To simplify the electron term in eq. (3), we assume $\xi_{0e} < 1$. Thus, the susceptibility for electron (eq. (3)) becomes

$$\chi_e \approx \frac{1}{k^2 \lambda_{De}^2} \left[1 + i\sqrt{\frac{\pi}{2}} \frac{(\omega - k_\| U_b)}{k_\| v_{te}} e^{-\xi_{0e}^2} \right]. \quad (6)$$

For the protons and doubly charged helium ions, we consider $\xi_{np,n\alpha} \gg 1$. Therefore, from eq. (1), $\chi_{p,\alpha}$ can be written as

$$\chi_{p,\alpha} \approx \frac{1}{k^2 \lambda_{Dp,\alpha}^2} \left[1 - \sum_{n=-\infty}^{\infty} \frac{\omega \Gamma_n(b_{p,\alpha})}{\omega - n\Omega_{p,\alpha}} \right.$$
$$\left. + i\sqrt{\frac{\pi}{2}} \sum_{n=-\infty}^{\infty} \frac{\omega \Gamma_n(b_{p,\alpha}) e^{-\xi_{np,\alpha}^2}}{k_\| v_{tp,\alpha}} \right]. \quad (7)$$

As proton cyclotron harmonics are being studied here, it is appropriate to assume $\omega \sim n\Omega_p$. Thus, the susceptibility of protons can be written as

$$\chi_p \approx \frac{1}{k^2 \lambda_{Dp}^2} \left[1 - \frac{\omega \Gamma_n(b_p)}{\omega - n\Omega_p} - G(b_p) \right.$$
$$\left. + i\sqrt{\frac{\pi}{2}} \sum_{n=-\infty}^{\infty} \frac{\omega \Gamma_n(b_p) e^{-\xi_{np}^2}}{k_\| v_{tp}} \right], \quad (8)$$

where the function $G(b_p) = \sum_{m \neq n} \omega \Gamma_m(b_p)/(\omega - m\Omega_p)$. The analytical expressions for $G(b_p)$ for $n = 1$ and 2 have been derived by Kindel and Kennel [5]. However, for higher harmonics, it is not easily tractable analytically, and therefore, has to be evaluated numerically. A computer program has been developed to

$$\Delta_p = \frac{\Gamma_n(b_p)}{1 + k^2\lambda_{Dp}^2 - \Gamma_n(b_p) - G(b_p) + \frac{T_p n_{0e}}{T_e n_{0p}}\left(1 - \frac{T_e z_\alpha^2 n_{0\alpha}}{T_\alpha n_{0e}}\right)}. \tag{14}$$

evaluate $G(b_p)$ in MATLAB and numerical results have been verified with the results obtained from the analytical expression obtained for fundamental mode. Thereafter, it has been applied to obtain the results for other harmonics.

Under the assumption $\omega \sim n\Omega_p$, susceptibility for helium ions is given by

$$\chi_\alpha \approx \frac{1}{k^2\lambda_{D\alpha}^2}\left[-1 + i\sqrt{\frac{\pi}{2}}\sum_{n=-\infty}^{\infty}\frac{\omega\Gamma_n(b_\alpha)e^{-\xi_{n\alpha}^2}}{k_\parallel v_{t\alpha}}\right], \tag{9}$$

where we have used $\Omega_\alpha = \Omega_p/2$ and $\sum_{n=-\infty}^{\infty}\Gamma_n(b_\alpha) = 1$. Combining eqs (6), (8) and (9), the dispersion relation for proton cyclotron mode can be written as

$$1 + \frac{1}{k^2\lambda_{De}^2}\left[1 + i\sqrt{\frac{\pi}{2}}\frac{(\omega - k_\parallel U_b)e^{-\xi_{0e}^2}}{k_\parallel v_{te}}\right]$$
$$+ \frac{1}{k^2\lambda_{D\alpha}^2}\left[-1 + i\sqrt{\frac{\pi}{2}}\sum_{n=-\infty}^{\infty}\frac{\omega\Gamma_n(b_\alpha)e^{-\xi_{n\alpha}^2}}{k_\parallel v_{t\alpha}}\right]$$
$$+ \frac{1}{k^2\lambda_{Dp}^2}\left[1 - \frac{\omega\Gamma_n(b_p)}{\omega - n\Omega_p} - G(b_p)\right]$$
$$+ \frac{1}{k^2\lambda_{Dp}^2}\left[i\sqrt{\frac{\pi}{2}}\sum_{n=-\infty}^{\infty}\frac{\omega\Gamma_n(b_p)e^{-\xi_{np}^2}}{k_\parallel v_{tp}}\right] = 0. \tag{10}$$

The real (D_r) and imaginary (D_i) parts of the dispersion relation (10) are as follows:

$$D_r = 1 + \frac{1}{k^2\lambda_{De}^2} - \frac{1}{k^2\lambda_{D\alpha}^2} + \frac{1 - G(b_p)}{k^2\lambda_{Dp}^2}$$
$$- \frac{\Gamma_n(b_p)}{k^2\lambda_{Dp}^2} - \frac{n\Omega_p}{\omega_r - n\Omega_p}\frac{\Gamma_n(b_p)}{k^2\lambda_{Dp}^2}, \tag{11}$$

$$D_i = \sqrt{\frac{\pi}{2}}\frac{1}{k^2\lambda_{De}^2}\frac{(\omega_r - k_\parallel U_b)e^{-\xi_{0e}^2}}{k_\parallel v_{te}}$$
$$+ \sqrt{\frac{\pi}{2}}\sum_{s=p,\alpha}\sum_{n=-\infty}^{\infty}\frac{1}{k^2\lambda_{Ds}^2}\frac{\omega_r\Gamma_n(b_s)e^{-\xi_{ns}^2}}{k_\parallel v_{ts}}. \tag{12}$$

Assuming that $\omega_r \sim n\Omega_p$, the real frequency can be obtained from eq. (11) and written in the following form:

$$\omega_r = n\Omega_p[1 + \Delta_p], \tag{13}$$

where

The assumption of $\omega_r \sim n\Omega_p$ is justified provided Δ_p is much smaller than 1. The growth/damping rates of proton cyclotron harmonics can be obtained by using the definition given by eq. (5), and is written below in a simplified form:

$$\frac{\gamma}{\Omega_p} = -n\Delta_p^2\frac{k^2\lambda_{Dp}^2}{\Gamma_n(b_p)}D_i. \tag{15}$$

For instability to grow $D_i < 0$. It must be noted that the damping due to the protons and helium ions is included in the analytical expression given by eq. (12). In the next subsection, analytical results on the helium cyclotron harmonics are presented.

2.2 *Helium cyclotron harmonics*

In this subsection, similar method is adopted as in the previous section to study the helium cyclotron harmonics. Therefore, at the outset, it is assumed that frequency $\omega \sim n\Omega_\alpha$. Thus, using the fact that $\Omega_p = 2\Omega_\alpha$ from eq. (7), the contribution of protons can be written in simplified form as

$$\chi_p = \frac{1}{k^2\lambda_{Dp}^2}\left[2 + i\sqrt{\frac{\pi}{2}}\sum_{n=-\infty}^{\infty}\frac{\omega\Gamma_n(b_p)}{k_\parallel v_{tp}}e^{-\xi_{np}^2}\right]. \tag{16}$$

Further, the corresponding term for helium ions is obtained as follows:

$$\chi_\alpha \approx \frac{1}{k^2\lambda_{D\alpha}^2}\left[1 - \frac{\omega\Gamma_n(b_\alpha)}{\omega - n\Omega_\alpha} - G(b_\alpha)\right.$$
$$\left. + i\sqrt{\frac{\pi}{2}}\sum_{n=-\infty}^{\infty}\frac{\omega\Gamma_n(b_\alpha)}{k_\parallel v_{t\alpha}}e^{-\xi_{n\alpha}^2}\right]. \tag{17}$$

The dispersion relation for helium cyclotron harmonics is obtained by combining eqs (6), (16), (17) and can be expressed as

$$1 + \frac{1}{k^2\lambda_{De}^2}\left[1 + i\sqrt{\frac{\pi}{2}}\frac{(\omega - k_\parallel U_b)}{k_\parallel v_{te}}e^{-\xi_{0e}^2}\right]$$

$$+ \frac{1}{k^2\lambda_{Dp}^2}\left[2 + i\sqrt{\frac{\pi}{2}}\sum_{n=-\infty}^{\infty}\frac{\omega\Gamma_n(b_p)}{k_\parallel v_{tp}}e^{-\xi_{np}^2}\right]$$

$$+ \frac{1}{k^2\lambda_{D\alpha}^2}\left[1 - \frac{\omega\Gamma_n(b_\alpha)}{\omega - n\Omega_\alpha} - G(b_\alpha)\right.$$

$$\left.+ i\sqrt{\frac{\pi}{2}}\sum_{n=-\infty}^{\infty}\frac{\omega\Gamma_n(b_\alpha)}{k_\parallel v_{t\alpha}}e^{-\xi_{n\alpha}^2}\right] = 0. \tag{18}$$

Here, the function $G(b_\alpha) = \sum_{m\neq n}\omega\Gamma_m(b_\alpha)/(\omega - m\Omega_\alpha)$ and imaginary part of eq. (18) are the same as eq. (12), whereas the real part is given by

$$D_r = 1 + \frac{1}{k^2\lambda_{De}^2} + \frac{2}{k^2\lambda_{Dp}^2}$$

$$+ \frac{1}{k^2\lambda_{D\alpha}^2}\left[1 - \frac{\omega\Gamma_n(b_\alpha)}{\omega - n\Omega_\alpha} - G(b_\alpha)\right]. \tag{19}$$

From eq. (19) the real frequency is obtained by equation $D_r = 0$ and is given by

$$\omega_r = n\Omega_\alpha[1 + \Delta_\alpha], \tag{20}$$

where

$$\Delta_\alpha = \frac{\Gamma_n(b_\alpha)}{1 + k^2\lambda_{D\alpha}^2 - \Gamma_n(b_\alpha) - G(b_\alpha) + \frac{T_\alpha n_{0e}}{z_\alpha^2 T_e n_{0\alpha}}\left(1 + 2\frac{T_e n_{0p}}{T_p n_{0e}}\right)}. \tag{21}$$

The assumption of $\omega_r \sim n\Omega_\alpha$ is justified provided Δ_α is much smaller than 1. The growth/damping rate for helium cyclotron modes can be written as

$$\frac{\gamma}{\Omega_\alpha} = -n\Delta_\alpha^2\frac{k^2\lambda_{D\alpha}^2}{\Gamma_n(b_\alpha)}D_i, \tag{22}$$

where D_i is given by eq. (12) and for the growth of the instability, $D_i < 0$. The theoretical results obtained here are general in nature and can be applied to laboratory or space plasmas. In the next section, numerical results will be presented on proton and cyclotron harmonic instabilities for the relevant plasma parameters. It emphasises that due to the assumptions $\omega \sim n\Omega_p$ and $\omega \sim n\Omega_\alpha$, $\xi_{np,n\alpha} \gg 1$, both protons and doubly charged helium ions are non-resonant. Therefore, our analysis is not valid when $\omega = n\Omega_p$ or $n\Omega_\alpha$ and then both ξ_{np} and $\xi_{n\alpha}$ would be $\ll 1$. Hence, the present analytical method avoids exact proton and helium cyclotron resonances. A different analytical approach is needed to deal with exact resonances. Further, in arriving at

analytical results, we have followed the well-established procedures laid down by Kindel and Kennel [5] and Rosenberg and Merlino [22].
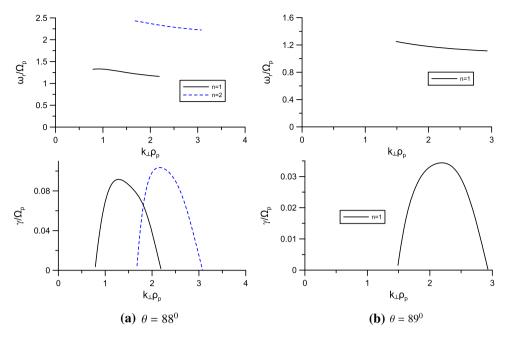
3. Numerical results

In this section, numerical results are shown pertaining to proton and helium cyclotron instabilities. The real frequency and growth rates for proton and helium cyclotron harmonics are obtained by solving eqs (13), (15) and (20), (22), respectively. We must mention here that, for the numerical results which are shown in §3.1 and 3.2, all the assumptions made in deriving the analytical results are satisfied. Furthermore, using plasma parameters from [40] (see their figure 2) and [22] (see their figure 1) and by putting the helium ion density to zero, we are able to confirm that the growth rate of the fundamental mode peaks near $k\rho_p \sim 1$ in both the cases. However, with an increase in angle of propagation, the growth rate peaks at $k\rho_p > 1$. Hence, we would like to emphasise that the peak growth rate is parameter-dependent and does not necessarily always peaks at $k\rho_p \sim 1$. It is important to mention here that while carrying out the numerical computations of the growth rate/damping of proton and helium harmonics, the dampings due to proton and helium ions have been taken into account.

3.1 *Proton cyclotron instability*

For proton cyclotron harmonics, we have normalised the various physical parameters in the following manner: frequencies are normalised with cyclotron frequency of proton, wave number with Larmor radius of proton $\rho_p = v_{thp}/\Omega_p$, electron beam speed by electron thermal velocity and the densities by total electron density at equilibrium. For numerical computations, the following fixed plasma parameters are used: $z_\alpha = 2$, $\omega_p/\Omega_p = 60$, $U_b/v_{te} = 0.80$, $n_{0\alpha}/n_{0e} = 0.10$, $m_p/m_\alpha = 0.25$, $m_p/m_e = 1837$, $T_e/T_p = 2$ and $T_\alpha/T_p = 2$.

In figure 1, the normalised frequency and normalised growth rates of proton cyclotron instability are shown with $k_\perp\rho_p$ for two different values of angle of propagation, θ. The results in the panels, i.e. figures 1a and 1b, are shown for $\theta = 88°$ and $89°$, respectively. Top and bottom panels of all the figures presented in this paper, respectively, show the real frequency and the corresponding growth rates of each harmonic denoted by n values in the figures. In the top left panel, two harmonics

Figure 1. Proton cyclotron instability: normalised real frequency (ω_r/Ω_p) and growth rate (γ/Ω_p) vs. $k_\perp\rho_p$ for $\theta = 88°$ (**a**) and 89° (**b**). Fixed plasma parameters are $z_\alpha = 2$, $\omega_p/\Omega_p = 60$, $U_b/v_{te} = 0.80$, $n_{0\alpha}/n_{0e} = 0.10$, $m_p/m_\alpha = 0.25$, $T_e/T_p = 2$ and $T_\alpha/T_p = 2$.

are plotted for which all the relevant conditions on electrons, protons and ions are satisfied. Here and in all subsequent figures, we are showing only growing modes. It can be seen that the growth rate of second harmonic ($\gamma/\Omega_p = 0.10$) is higher than that of the fundamental harmonic ($\gamma/\Omega_p = 0.092$) for $\theta = 88°$. In this figure and in all subsequent figures, curves are restricted to wave number ranges where growth rates are positive. The peak growth of fundamental harmonic occurs at $k_\perp\rho_p \approx 1.29$ with $\omega_r \approx 1.29\Omega_p$ and the absolute value of the argument of plasma dispersion function for protons is $(\omega - \Omega_p)/\sqrt{2}k_\parallel v_{tp} \approx 4.51$, and it is larger for lower wave numbers and decreases with increasing wave numbers. This pattern is seen for all the harmonics. Although not shown here, when the angle of propagation is increased to $\theta = 88.5°$, then also two harmonics become unstable. But, in this case, the maximum growth rate of both harmonics decreases and the value of fundamental mode reaches $\gamma/\Omega_p = 0.0617$ and that of second harmonic reaches $\gamma/\Omega_p = 0.0619$. When the angle of propagation is increased to $\theta = 89°$ (figure 1b), the growth rate is seen only for the first harmonic and maximum growth rate becomes $\gamma/\Omega_p \approx 0.034$ at $k\rho_p \approx 2.19$. So it can be seen that the growth rate for fundamental harmonics decreases with the increase in angle of propagation.

We have analysed the effect of electron streaming on the proton cyclotron harmonics in figure 2 on the normalised real frequency and growth rates for the parameters of figure 1a with the angle of propagation

$\theta = 88°$. The results are displayed in two panels, i.e. in figure 2a ($U_b/v_{te} = 0.6$) and in figure 2b ($U_b/v_{te} = 0.7$). It can be seen that for $U_b/v_{te} = 0.6$ (figure 2a), only first two harmonics can be excited, with the peak value of growth rate of fundamental harmonic being 0.047 at $k\rho_p \sim 1.58$. Here, the growth rate of the first harmonic is higher than that of the second harmonic. On the other hand, for $U_b/v_{te} = 0.7$ (figure 2b), it is observed that two harmonics are excited with growth rate of the second harmonic greater than that of the first harmonic. This trend continues for $U_b/v_{te} = 0.8$ (refer to figure 1a), where, again, only two modes become unstable. The peak value of the growth rate for each harmonic increases with an increase in the value of electron beam speed. It is also found that for each harmonic, the peak value of the growth rate occurs at smaller values of $k\rho_p$, e.g. the peak value of γ/Ω_p for fundamental harmonic for $U_b/v_{te} = 0.6$, 0.7 and 0.8 occurs at $k\rho_p \sim 1.58$, ~ 1.42, ~ 1.29, respectively. This is also true for all other harmonics. In the next subsection, the numerical results on helium cyclotron instability are discussed.

Although not shown here, we have studied the effect of variations of $n_{0\alpha}/n_{0e}$ on proton cyclotron real frequency and growth rate for $\theta = 88°$. It is found that increasing $n_{0\alpha}/n_{0e}$ from 0.08 to 0.12 tends to slightly increase the growth rate. The numerical computations show that for proton harmonics, the contribution of the helium damping is negligible. However, damping due to protons reduces with the increase in the number density
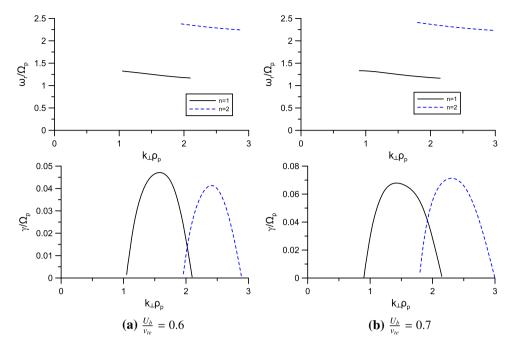
Figure 2. Proton cyclotron instability: normalised real frequency and growth rate vs. $k_\perp \rho_p$ for $U_b/v_{te} = 0.6$ (**a**) and 0.7 (**b**). Other fixed plasma parameters are the same as in figure 1a.
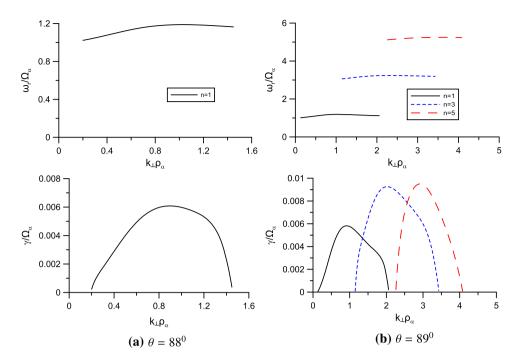
of the helium ions. Thus, the growth rate increases with increase in the number density of the helium ions. We have also studied the effect of the variation of T_α/T_p on the real frequency and growth rate (not shown here) for the parameters of figure 1a, for $T_\alpha/T_p = 4$ and 6 and the angle of propagation is $\theta = 88°$. It is observed that the growth decreases slightly with the increase in T_α/T_p.

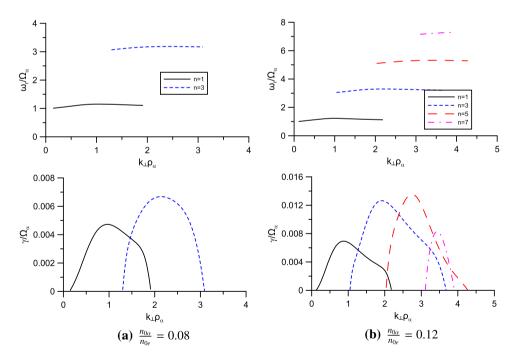### 3.2 *Helium cyclotron instability*

In this subsection, the effect of various parameters on helium cyclotron instability is studied. The frequencies are normalised with helium cyclotron frequency and wave number with Larmor radius of helium $\rho_\alpha = v_{th\alpha}/\Omega_\alpha$. Other normalisations are the same as in §3.1. Here we have plotted the real frequency and growth rates vs. $k_\perp \rho_\alpha$. The curves have been limited by the plasma conditions imposed on the argument of plasma dispersion function or wherever the damping occurs.

In figures 3a and 3b, the normalised real frequency and growth rates are plotted for $\theta = 88°$ and $89°$, respectively. The fixed plasma parameters are $z_\alpha = 2$, $\omega_p/\Omega_p = 60$, $U_b/v_{te} = 0.80$, $n_{0\alpha}/n_{0e} = 0.10$, $m_p/m_\alpha = 0.25$, $m_p/m_e = 1837$, $T_e/T_p = 10$ and $T_\alpha/T_p = 0.2$. An interesting feature of helium harmonic is that for all the variations that had been undertaken, only the odd harmonics are getting exited, unless stated otherwise. Generally, the even harmonics of the helium cyclotron waves are not excited due

to the proton cyclotron damping at these frequencies. For instance, consider the case of $\theta = 88°$ (figure 3a). Here, only first harmonic is excited with its growth rate peaking at $k_\perp \rho_\alpha \approx 0.9$ with a value of $\gamma/\Omega_\alpha \approx 0.006$ and $\omega/\Omega_\alpha \approx 1.18$. Also, here the growth of the wave is for wider range of wave numbers compared to that of proton harmonics discussed in the previous sections. Although, not shown here, when the angle is increased to $\theta = 88.5°$, the first and third harmonics get excited with third harmonic having larger growth rate than the first harmonic. As the angle is increased to $\theta = 89°$, the first, third and fifth harmonics are excited (figure 3b). Also, with an increasing value of angle of propagation, the peak growth rate occurs at higher value of $k_\perp \rho_\alpha$. The peak growth rate for fundamental harmonic of helium for $\theta = 89°$ is $\gamma/\Omega_\alpha \approx 0.0058$ at $k_\perp \rho_\alpha \approx 0.92$. The corresponding absolute value of the argument of the plasma dispersion function is $(\omega - \Omega_{p\alpha})/\sqrt{2}k_\parallel v_{t\alpha} \approx 8.14$, whereas it is larger for lower values of wave numbers and decreases with an increasing wave number. This pattern is seen for all the results presented. For further increase in angle of propagation to $\theta = 89.5°$, the first, second, third, fifth, seventh and ninth harmonics can be excited (not shown here).

In figure 4, the real frequency and growth rate are plotted for $n_{0\alpha}/n_{0e} = 0.08$ (figure 4a) and 0.12 (figure 4b) for parameters of figure 3b with $\theta = 89°$. For $n_{0\alpha}/n_{0e} = 0.08$, the fundamental mode and third mode can be excited. However, for $n_{0\alpha}/n_{0e} = 0.10$ (figure 3b), the first, third and fifth harmonics can be
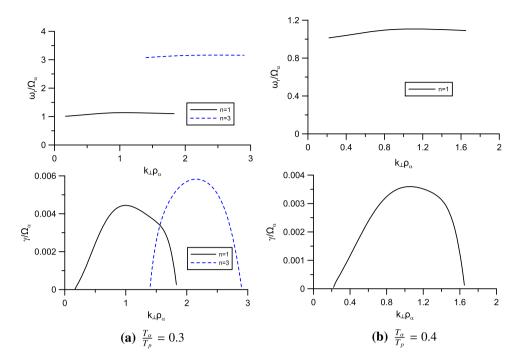
Figure 3. Helium cyclotron instability: normalised real frequency ω_r / Ω_α and growth rate γ / Ω_α vs. $k_\perp \rho_\alpha$ for $\theta = 88°$ (**a**) and 89° (**b**). Fixed plasma parameters are $z_\alpha = 2$, $\omega_p/\Omega_p = 60$, $U_b/v_{te} = 0.80$, $n_{0\alpha}/n_{0e} = 0.10$, $m_p/m_\alpha = 0.25$, $T_e/T_p = 10$ and $T_\alpha/T_p = 0.2$.
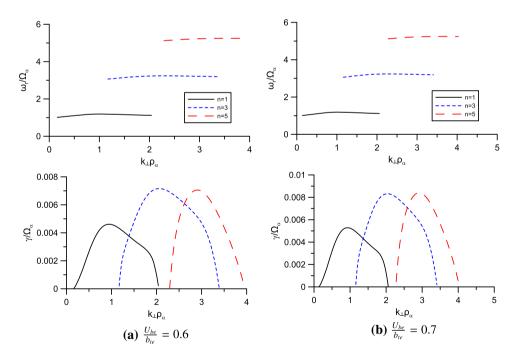

Figure 4. Helium cyclotron instability: normalised real frequency and growth rate vs. $k_\perp \rho_\alpha$ for $n_{0\alpha}/n_{0e} = 0.08$ (**a**) and 0.12 (**b**). Other fixed plasma parameters are the same as in figure 3b.

excited. Finally, for $n_{0\alpha}/n_{0e} = 0.12$, the first, third, fifth and seventh harmonics are excited. It is important to mention here that the growth rate increases substantially with the increase in helium ion density. The numerical computations show that for odd helium harmonics,

the contribution of the proton damping is negligible. However, damping due to helium ions reduces with the increase in the number density of the helium ions. Thus, the growth rate of helium harmonics increases with an increase in the number density of the helium

Figure 5. Helium cyclotron instability: normalised real frequency and growth rate vs. $k_\perp \rho_\alpha$ for $T_\alpha/T_p = 0.3$ (**a**) and 0.4 (**b**). Other fixed plasma parameters are the same as in figure 3b.

Figure 6. Helium cyclotron instability: normalised real frequency and growth rate vs. $k_\perp \rho_\alpha$ for $U_{be}/b_{te} = 0.6$ (**a**) and 0.7 (**b**). Other fixed plasma parameters are the same as in figure 3b.

ions. The variation of T_α/T_p on the helium cyclotron instability is shown in figure 5 for the parameters of figure 3b with $\theta = 89°$ for $T_\alpha/T_p = 0.3$ (figure 5a) and $T_\alpha/T_p = 0.4$ (figure 5b). It is observed that the growth rate decreases with an increase in helium

ion temperature. Also, the number of harmonics that is getting excited decreases with an increase in the helium ion temperature. In figure 6, the effect of variation of electron beam speed is shown on the helium cyclotron instability. It can be seen that for $U_b/v_{te} = 0.6$

(figure 6a), $U_b/v_{te} = 0.7$ (figure 6b) and $U_b/v_{te} = 0.8$ (figure 3b), the first, third and fifth harmonics are excited with an increase in the peak growth rate.

4. Discussions and conclusions

EIC instability associated with higher harmonics of proton and helium cyclotron modes has been investigated. The magnetised plasma consists of three components: beam electron, protons and doubly charged helium ions. The effect of various plasma parameters such as angle of propagation, number density and temperature of helium ions and electron beam speed has been studied on the growth of proton and helium cyclotron instability. In this study, we employed the method adopted by Kindel and Kennel [5] and later on used by Rosenberg and Merlino [22] to study the higher harmonics of EIC waves. However, the method cannot be applied at the exact proton and helium harmonics, i.e. $\omega = n\Omega_p$ and $n\Omega_\alpha$.

It is found that growth rates decrease for both proton harmonics and helium harmonics with an increase in the angle of propagation. However, a fewer number of proton harmonics and higher number of helium harmonics are excited when the angle of propagation is increased. The conclusions drawn here are valid for both proton and helium cyclotron instabilities. The extent of wave number for which both the proton and helium harmonics are unstable increases with an increase in angle of propagation and the peak growth rate occurs at higher wave number. The increase in number density of ions enhances the growth of the instability. However, the temperature of ions has inverse effect on the instability. Further, as the electron beam speed is increased, the number of excited harmonics increases and the peak growth rate also increases and occurs at a larger value of wave number.

Cluster observations of EIC waves in the nightside auroral region at $4R_E$ have been reported by Backrud-Ivgren *et al* [41]. They pointed out that these waves can be generated by electron beams. The total density of electrons was estimated to be 5 cm^{-3} and proton cyclotron frequency is 7.6 Hz. If we consider all ions as protons with small fraction of helium ions, then $\omega_p/\Omega_p \approx 60$ which we have assumed in our numerical calculations of all the figures presented in this paper. For proton as well as helium growth rate and real frequency calculations, we have taken $U_b/v_{te} = 0.8$. For the plasma parameters used in figure 1a, the peak growth rate of proton cyclotron fundamental mode comes out to be 700 mHz at $k_\perp\rho_p \approx 1.29$ and the corresponding frequency is $\omega_r \approx 1.28\Omega_p = 9.7$ Hz. Similarly, for helium cyclotron fundamental mode (figure 3a), the

peak growth rate is $\approx$23 mHz at $k_\perp\rho_\alpha \approx 0.9$ with the corresponding frequency $\omega_r \approx 1.18\Omega_\alpha = 4.84$ Hz.

In the auroral region, the EIC waves accelerate the ions in the direction perpendicular to the magnetic field of the Earth and the ions are driven upward into the magnetosphere. Hence, this mechanism is believed to be one of the primary source of heavy ions in the magnetosphere [42,43]. Further, EIC waves have the lowest thresholds of excitation among various current-driven instabilities. Very recently, Tang *et al* [34] have conducted an extensive study of large-amplitude EIC waves near Earth's dayside magnetopause and have concluded that the presence of EIC waves in the magnetopause boundary layer may contribute to maintaining the boundary layers. Here, we have given an example of the auroral region where our results can be applied. The theory developed here is general in nature and can be applied to EIC observations in laboratory plasmas [44] as well as space plasmas [34,41,45]. For example, our method can be applied to study the first and second harmonics of proton and fundamental harmonic of helium cyclotron modes observed by the THEMIS satellite in the magnetopause [34]. We are trying to get the relevant plasma parameters for THEMIS observations and the results will be reported elsewhere.

The role of EIC instability in the heating of solar corona was studied by Hinata [46] and Luhn [47]. Hinata [46] has shown that coronal plasma is heated up to a temperature of a few million Kelvin degrees when the electron drift velocity is near or above the critical value of EIC instability. Similarly, Luhn [47] has studied the selective heating of minority ion species in the corona by using EIC waves. Luhn [47] has shown that in certain region of phase space, depending upon the initial condition of nonlinearly coupled system of waves and gyrating ions, the energy transfer takes place between particles and waves, which results in heating of particle distribution. Therefore, it will be interesting to know whether the recently launched Parkar Solar Probe can measure the ion heating associated with EIC waves, and verify the theoretical predictions.

References

[1] N D'Angelo and R W Motley, *Phys. Fluids* **5**, 633 (1962)
[2] R W Motley and N D'Angelo, *Phys. Fluids* **6**, 296 (1963)

[3] W E Drummond and M N Rosenbluth, *Phys. Fluids* **5**, 1507 (1962)

[4] E S Weibel, *Phys. Fluids* **13**, 3003 (1970)

[5] J M Kindel and C F Kennel, *J. Geophys. Res.* **76**, 3055 (1971)

[6] K F Lee, *J. Plasma Phys.* **8**, 379 (1972)

[7] F W Perkins, *Phys. Fluids* **19**, 1012 (1976)

[8] M Yamada, S Seiler, H W Hendel and H Ikezi, *Phys. Fluids* **20**, 450 (1977)

[9] P M Kintner, M C Kelley, R D Sharp, A G Ghielmetti, M Temerin, C Cattell, P F Mizera and J F Fennell, *J. Geophys. Res.* **84**, 7201 (1979)

[10] C Cattell, *J. Geophys. Res.* **86**, 3641 (1981)

[11] H Okuda and K-I Nishikawa, *J. Geophys. Res.* **89**, 1023 (1984)

[12] G S Lakhina, *J. Geophys. Res.* **92**, 12161 (1987)

[13] G Ganguli, S Slinker, V Gavrishchaka and W Scales, *Phys. Plasmas* **9**, 2321 (2002)

[14] M J Kurian, S Jyothi, S K Leju, M Isaac, C Venugopal and G Renuka, *Pramana – J. Phys.* **73**, 1111 (2009)

[15] M Barati Moqadam Niyat, S M Khorashadizadeh and A R Niknam, *Phys. Plasmas* **23**, 122110 (2016)

[16] B Song, D Suszcynsky, N D'Angelo and R L Merlino, *Phys. Fluids B* **1**, 2316 (1989)

[17] C Venugopal, P J Kurian and G Renuka, *Pramana – J. Phys.* **37(3)**, 303 (1991)

[18] A Barkan, N D'Angelo and R L Merlino, *Planet. Space Sci.* **43**, 905 (1995)

[19] V W Chow and M Rosenberg, *Planet. Space Sci.* **43**, 613 (1995)

[20] V W Chow and M Rosenberg, *Phys. Plasmas* **3**, 1202 (1996)

[21] S-H Kim, J R Heinrich and R L Merlino, *Planet. Space Sci.* **56**, 1552 (2008)

[22] M Rosenberg and R L Merlino, *J. Plasma Phys.* **75**, 495 (2009)

[23] J Sharma, S C Sharma, V K Jain and A Gahlot, *J. Plasma Phys.* **79**, 577 (2013)

[24] A K Chattopadhyay, S V Kulkarni and R Srinivasan, *Pramana – J. Phys.* **85(4)**, 713 (2015)

[25] S R Mosier and D A Gurnett, *Nature* **223**, 605 (1969)

[26] P M Kintner, M C Kelley and F S Mozer, *Geophys. Res. Lett.* **5**, 139 (1978)

[27] M Temerin, M Woldorff and F S Mozer, *Phys. Rev. Lett.* **43**, 1941 (1979)

[28] D T Young, S Perraut, A Roux, C de Villedary, R Gendrin, A Korth, G Kremser and D Jones, *J. Geophys. Res.* **86**, 6755 (1981)

[29] A Roux, S Perraut, J L Rauch, C de Villedary, G Kremser, A Korth and D T Young, *J. Geophys. Res.* **87**, 8174 (1982)

[30] C A Cattell, F S Mozer, I Roth, R R Anderson, R C Elphic, W Lennartsson and E Ungstrup, *J. Geophys. Res.* **96**, 11421 (1991)

[31] M André, H Koskinen, G Gustafsson and R Lundin, *Geophys. Res. Lett.* **14**, 463 (1987)

[32] F S Mozer, R Ergun, M Temerin, C Cattell, J Dombeck and J Wygant, *Phys. Rev. Lett.* **79(7)**, 1281 (1997)

[33] C Cattell, R Bergmann, K Sigsbee, C Carlson, C Chaston, R Ergun, J McFadden, F S Mozer, M Temerin, R Strangeway, R Elphic, L Kistler, E Moebius, L Tang, D Klumpar and R Pfaff, *Geophys. Res. Lett.* **25**, 2053 (1998)

[34] X Tang, C Cattell, R Lysak, L B Wilson, L Dai and S Thaller, *J. Geophys. Res.* **120**, 3380 (2015)

[35] D R Dakin, T Tajima, G Benford and N Rynn, *J. Plasma Phys.* **15**, 175 (1976)

[36] E Ungstrup, D M Klumpar and W J Heikkila, *J. Geophys. Res.* **84**, 4289 (1979)

[37] R D Sharp, R G Johnson and E G Shelly, *J. Geophys. Res.* **79**, 5167 (1974)

[38] T Sreeraj, S V Singh and G S Lakhina, *Phys. Plasmas* **23(8)**, 082901 (2016)

[39] T Sreeraj, S V Singh and G S Lakhina, *Phys. Plasmas* **25(5)**, 052902 (2018)

[40] H Okuda, C Z Cheng and W W Lee, *Phys. Fluids* **24**, 1060 (1981)

[41] M Backrud-Ivgren, G Stenberg, M André, M Morooka, Y Hobara, S Joko, K Rönnmark, N Cornilleau-Wehrlin, A Fazakerley, A Rème, H Fazakerley and H Rème, *Ann. Geophys.* **23**, 3739 (2005)

[42] J L Horwitz, *Rev. Geophys.* **20(4)**, 929 (1982)

[43] L A Frank, K L Ackerson and D M Yeager, *J. Geophys. Res.* **82(1)**, 129 (1977)

[44] D M Suszcynsky, N D'Angelo and R L Merlino, *J. Geophys. Res.* **94**, 8966 (1989)

[45] V V Gavrishchaka, G I Ganguli, W A Scales, S P Slinker, C C Chaston, J P McFadden, R E Ergun and C W Carlson, *Phys. Rev. Lett.* **85**, 4285 (2000)

[46] S Hinata, *Astrophys. J.* **235**, 258 (1980)

[47] A Luhn, *Adv. Space Res.* **4(2–3)**, 165 (1984)